

Short Communication

# An Electrochemical Investigation of Corrosion Behavior of 316L Austenitic Stainless Steel Reinforcement in Concrete Exposed to Acidic Environment

Chunjiao Chen<sup>1</sup>, Jingwu Zuo<sup>2,\*</sup>, Yingjie Wang<sup>3</sup>

<sup>1</sup> School of Architecture, South China University of Technology, Guangzhou 510641, China

<sup>2</sup> School of Engineering Technology, Beijing Normal University, Zhuhai, 519087, China

<sup>3</sup> China Water Resources Pearl River Planning, Survey

& Designing Co., Ltd. Guangzhou, 510610, China

\*E-mail: [zuojingwubnu@163.com](mailto:zuojingwubnu@163.com)

Received: 4 October 2019/ Accepted: 25 November 2019 / Published: 31 December 2019

---

Steel reinforced concrete has the potential to withstand a variety of adverse environmental conditions. Nowadays, corrosion in reinforced concrete is highly regarded due to the durability of the structures. In this research, concrete cubes containing 50 wt.% Limestone and reinforced with 316L austenitic and 2304 duplex stainless steels were subjected to study on corrosion behavior in 0.5 M H<sub>2</sub>SO<sub>4</sub> solution using open-circuit potential and electrochemical impedance spectroscopy techniques. The corrosion current density of the 316L austenitic and 2304 duplex steels were 0.052 and 0.063 μA/cm<sup>2</sup>, respectively, which determined by potentiodynamic polarization diagrams. These results show that both steel reinforced concretes remained completely in the passive state during the test which indicates their good corrosion resistance in the acidic environment. Niquist diagram of the 316L austenitic stainless steel rebar indicates only an incomplete capacitive semi-circle, indicating the formation of a passive layer with a high protective property. An inductive behavior at high frequency was observed for 2304 duplex steel. Scanning electron microscope image indicates that 316L austenitic stainless steel surface was without evidence of pores/defects and unevenness which can reduce the influence of aggressive ions and moisture on the surface.

---

**Keywords:** Stainless steel reinforced concrete; Corrosion resistance; 316L austenitic stainless steel; Electrochemical impedance spectroscopy; Corrosive environment

## 1. INTRODUCTION

Reinforced concrete has the potential to withstand a variety of adverse environmental conditions [1]. Steel in reinforced concrete provides the tensile properties required in structural concrete [2]. Corrosion in reinforced concrete due to the durability of the structure has received much attention [3]. Corrosion is the gradual degradation of materials due to chemical reaction with the

environment, which consists electrochemical reactions that is dependent on the transportation of electrons to the adjacent materials [4]. To improve the durability of concrete structures, researchers and engineers have done a great deal of research. Currently, there are numerous strategies to extend the lifespan of reinforced structures exposed to corrosive environments, including the corrosion inhibitors, corrosion resistant steel, protective coatings on steel reinforcement and non-ferrous reinforcement [5-8]. Some researchers have already started using stainless steel rebar under severe corrosive environment conditions. Stainless steel compared to carbon steel can significantly improve chloride thresholds and prolong the initial stage of rebar corrosion in concrete [9].

Among the different types of stainless steel, austenitic stainless steels are molybdenum-bearing austenitic stainless steels or a low-carbon austenitic stainless steel with Molybdenum which have low nickel content, no molybdenum and the large amount of manganese is making them cheaper than the other stainless steels while retaining the austenitic structure [10]. The chromium element makes the corrosion resistance on the surface of rebar by creating a protective film [11]. Many electrochemical measurement methods have been considered to determine the corrosion behavior of steel in concrete. Electrochemical techniques including potential mapping, electrochemical impedance spectroscopy (EIS), potentiodynamic and potentiostatic are generally used to measure the reinforcing steel corrosion [12, 13].

Here, the corrosion behavior of 316L austenitic stainless steel rebar were investigated and compared with 2304 duplex steel rebar using electrochemical technique in acidic environment. Electrochemical Impedance Spectroscopy (EIS) was used to assess the corrosion resistance of steel rebars.

## 2. MATERIALS AND METHODS

In this work, Cubes of ordinary Portland cement reinforced with 316L austenitic or 2304 duplex steel rebars with 6 mm diameter and 10 cm length were employed. Chemical composition of 316L austenitic and 2304 duplex stainless steels which were used as rebar in this work are shown in table 1.

**Table 1.** Chemical composition of 316L austenitic and 2304 duplex stainless steel rebar (wt%)

Steel type	Fe	C	Mn	Si	S	P	Cr	Ni	Mo	N
2304 duplex stainless steel	72.7	0.02	0.00	0.00	0.001	0.00	23.03	4	0.00	0.1
316L austenitic stainless steel	64.9	0.03	1.3	0.47	0.03	0.03	17.4	13.4	2.32	0.09

The cement was prepared by the combination of 50 wt% Clay/Shale/Sand and 50 wt% Limestone at furnace temperature of 1200 °C through 540 kg CO<sub>2</sub>/t and 3.6 GJ energy/t of cement. Concrete was made using cement with 0.40 water/cement ratio. Mortar cubes were made with a similar proportion which had cement, sand and gravel with the ratio of 1:2:4. The reinforced concrete samples were positioned at an environmental chamber at room temperature to accelerate the corrosion process of the steel bar. 0.5 M H<sub>2</sub>SO<sub>4</sub> solutions were utilized to assess the corrosion behavior of steel reinforced concretes in acidic environment. EIS characterizations were done in the frequency between 100 kHz and 100 μHz at the open circuit potential (OCP) with AC perturbation ±10 mV. DC polarization experiments were done from -0.8 V to +1.0 V vs. OCP at 1 mV/s scan rate. The surface morphology of steel rebars were characterized by scanning electron microscopy (SEM; FEI/Nova NanoSEM 450).

### 3. RESULTS AND DISCUSSION

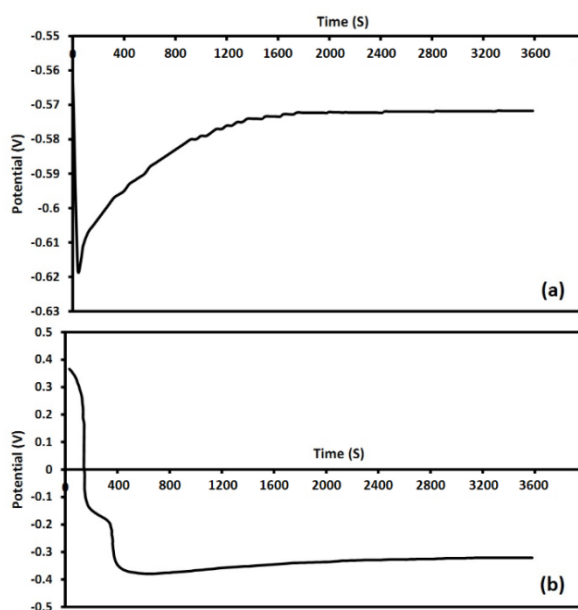


**Figure 1.** Open circuit potential plots of (a) 2304 duplex and (b) 316L austenitic stainless steel reinforcements

The diagrams of open-circuit potential (OCP) variations for 316L austenitic and 2304 duplex stainless steel reinforced concretes in 0.5 M sulfuric acid (H<sub>2</sub>SO<sub>4</sub>) solution are shown in figure 1. As shown in the figure, at the beginning of immersion, the potentials of both steels decrease rapidly, indicating the dissolution of the oxide layer formed on the steel surface in an acidic environment. But over time, the potential shifts to positive values. This trend has also been reported for other austenitic stainless steels in similar acidic environments [14]. This behavior reflects the formation of the passive layer which its protective role increased during the immersion time [15]. Moreover, a completely steady state was obtained after placing the working electrodes in acidic solution for 60 min.

Figure 2 indicates potentiodynamic polarization diagrams of 316L austenitic and 2304 duplex stainless steel rebars immersed in 0.5 M H<sub>2</sub>SO<sub>4</sub> solution for 60 min in OCP conditions. As shown in

figure 2, the anodic branches of experimental polarization curves are characterized by passive regions at both reinforcement steels, demonstrating that the passive layers have clearly formed on the surface of rebar when they are immersed to the corrosive electrolyte [16]. It can also be seen that a significant shift of corrosion potential towards a positive direction, suggesting that the anodic metal dissolution retarded efficiently by 316L austenitic stainless steel [17]. As compared to the 2304 duplex rebar, the passive region is much wider at the 316L austenitic steel rebar, and the passive current density is about  $0.01\mu\text{A}/\text{cm}^2$  lower than that of the 2304 duplex stainless steel, demonstrating the corrosion resistance in the passivated steel is enhanced for 316L austenitic steel rebar.

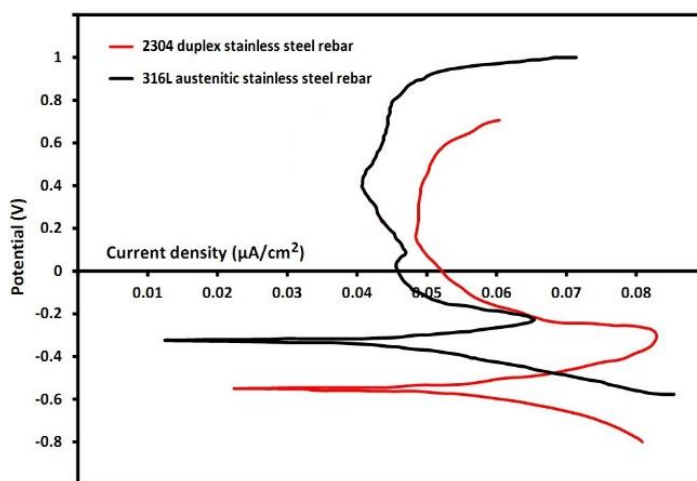


**Figure 2.** Potentiodynamic polarisation of 316L austenitic and 2304 duplex stainless steel reinforced concretes in 0.5 M sulfuric acid.

**Table 2.** Corrosion current density and potential of the stainless steel rebars

Steel type	Corrosion current density	Corrosion potential
2304 duplex stainless steel	$0.063 \mu\text{A}/\text{cm}^2$	-0.54 V
316L stainless steel	$0.052 \mu\text{A}/\text{cm}^2$	-0.33 V

The values of corrosion current density and corrosion potential are shown in table 2 which is obtained from the potentiodynamic polarization diagrams in Figure 2.

The corrosion level can be defined into four levels proposed by Durar Network Specification [18]: very high corrosion for  $1.0 \mu\text{A}/\text{cm}^2 < i_{\text{corr}}$ , high corrosion for  $0.5 \mu\text{A}/\text{cm}^2 < i_{\text{corr}} < 1.0 \mu\text{A}/\text{cm}^2$ , low corrosion for  $0.1 \mu\text{A}/\text{cm}^2 < i_{\text{corr}} < 0.5 \mu\text{A}/\text{cm}^2$ , and passivity for  $i_{\text{corr}} < 0.1 \mu\text{A}/\text{cm}^2$ . As shown in table 2, the corrosion current density of the 316L austenitic steel, in 0.5 M  $\text{H}_2\text{SO}_4$  solution, is  $0.052 \mu\text{A}/\text{cm}^2$ . However, the corrosion current density of 316L austenitic steel in this acidic environment is in the range of  $0.052 \mu\text{A}/\text{cm}^2$ , which is lower than that of 2304 duplex stainless steel. Therefore, both steel reinforced concretes at  $\text{H}_2\text{SO}_4$  solution remained completely in the passive state during the test which indicates their good corrosion resistance in the acidic environment [19]. The corrosion monitoring reveals that the corrosion rate of 316L austenitic and 2304 duplex stainless steel rebars estimated to be

0.4 and 0.7  $\mu\text{m year}^{-1}$ , respectively. The lower corrosion rate of 316L austenitic rebar can be attributed to the percent compositions Mo along with greater percentages of Ni and Cr, which makes it more resistant to corrosion and one of the most widely used stainless steel alloys in reinforced concretes. Furthermore, the resistance to pitting corrosion and passive film breakdown can be controlled by the use of Mo and Ni.

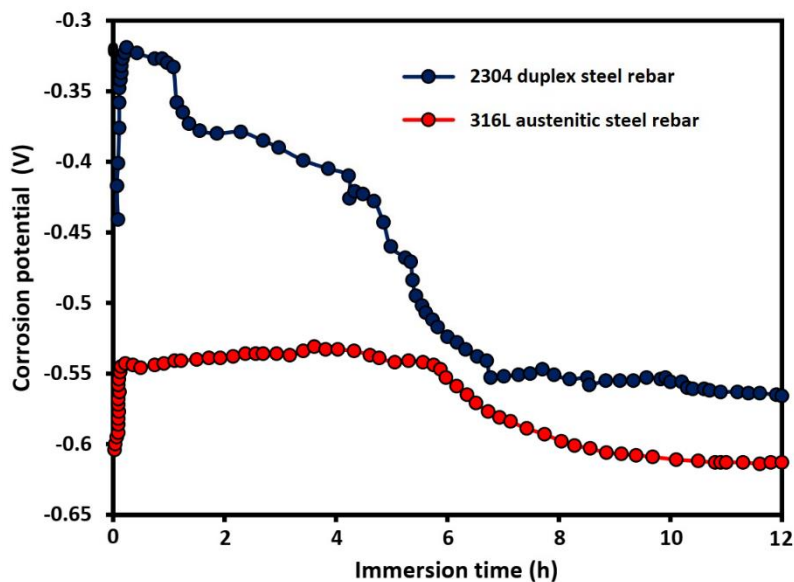


**Figure 3.** Corrosion potential of stainless steel rebars immersed in 0.5 M  $\text{H}_2\text{SO}_4$  solution.

Figure 3 indicates the corrosion potential of stainless steel rebars immersed for 12 h in 0.5 M  $\text{H}_2\text{SO}_4$  solution. As shown, the OCP in the 2304 duplex steel quickly increases to -0.32 V and approximately maintains for 4 h. Then, the potential decreases sharply to -0.54 V. In the 316L austenitic steel rebar, the OCP also rapidly increases to -0.54 V and then the potential decreases suddenly to -0.62 V in the final phase after 6 h. The change of OCP may reveal the electrochemical behavior of the surface of steel rebar. The passive state usually relates to a high potential region while the active state relates to a low potential region [20]. Therefore, the passive film formed on the surface of 2304 duplex steel can be maintained for 4 h in the acidic solution, and then destroyed by breaking or pitting. However, the passive stage is increased to 6 h in the 316L austenitic steel. Meanwhile, the reduction of passive state stainless steel to active state at OCP becomes slower in 316L austenitic steel rebar. Moreover, there are OCP transient fluctuations before the sharp reduction of both rebar in acidic solution, indicating the repassivation and formation of microscopic pits.

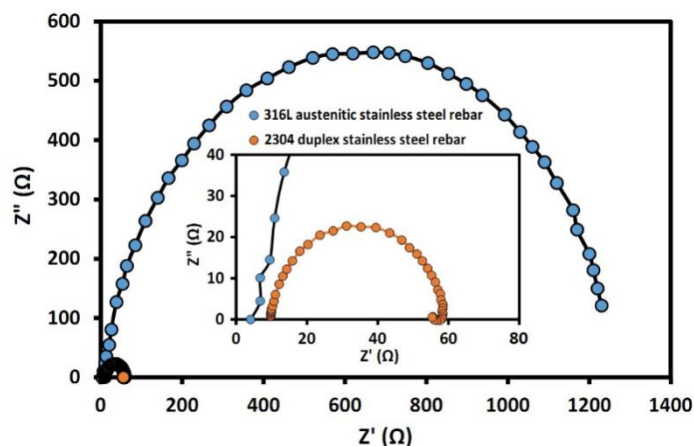


**Figure 4.** Nyquist diagrams of 316L austenitic and 2304 duplex stainless steel reinforced concretes in 0.5 M sulfuric acid after one-hour immersion time

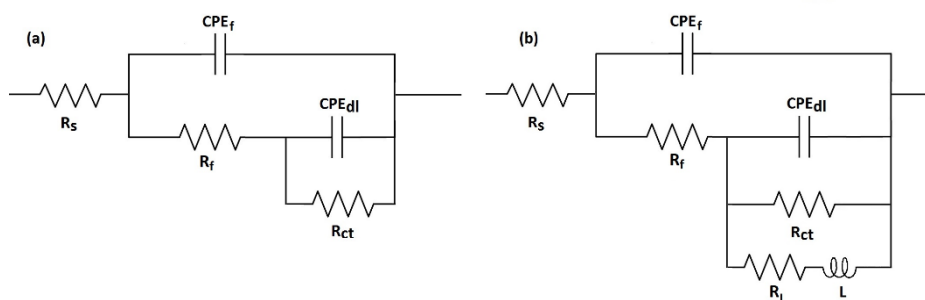


**Figure 5.** Equivalent circuits used to fit the EIS

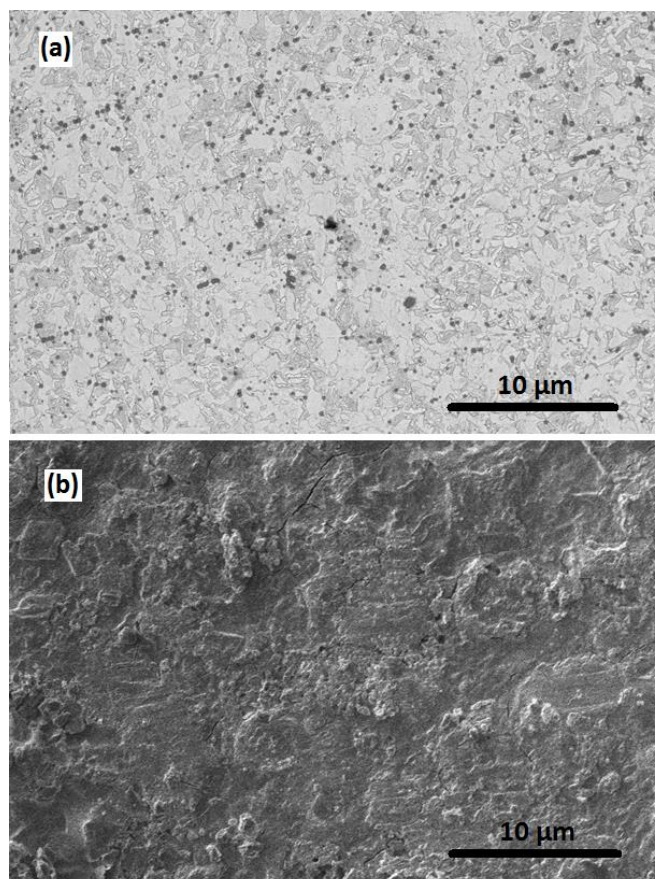
In order to describe corrosion behavior of the stainless steel reinforced concretes, EIS spectra was performed after 60 min exposure time. Figure 4 reveals the Niquistplots obtained by EIS of 316L austenitic and 2304 duplex stainless steel in 0.5 M  $H_2SO_4$  solution in OCP conditions. As shown in Fig. 4, in the high and mid-frequency range, a capacitive loop is followed, and at low frequencies, an inductive behavior is observed for 2304 duplex steel [21]. However, the Niquist diagram of the 316L austenitic stainless steel reinforcement indicates only an incomplete capacitive semi-circle, indicating the formation of a passive layer with a high protective property.

Generally, an electrochemical phenomenon can be studied by obtaining its impedance equation. For example, the impedance spectrum is modeled with a suitable circuit and the experimental spectrum is adapted to obtain the values corresponding to the equivalent circuit. Then, these values are associated to a chemical-physical phenomenon to prove that the resulting equivalent circuit is an acceptable representation of the phenomena occurring. Equivalent circuits of Figures 5a and 5b were used to model the Nyquist diagrams for 316L austenitic and 2304 duplex steels, respectively.

In these equivalent circuits, the  $CPE_f$  and  $R_f$  are constant-phase element and resistance of passive film, respectively.  $CPE_{dl}$  and  $R_{ct}$  are constant-phase element and charge-transfer resistance, respectively.  $R_s$  is the resistance of solution [22].  $L$  and  $R_L$  represent the equivalent inductance and resistance. The presence of inductance for the 2304 duplex steel sample exposed to acidic solution is due to the partial breakdown of the passive film and an initial deterioration process [23].

**Table 3.** Electrochemical parameters from the equivalent circuit in Figure 5 for stainless steel rebars

Steel type	$R_s(\Omega \text{ cm}^2)$	$CPE_f(\mu\text{F cm}^{-2})$	$R_f(\Omega \text{ cm}^2)$	$R_{ct}(\Omega \text{ cm}^2)$	$CPE_{dl}(\mu\text{F cm}^{-2})$	$L(\text{Hcm}^2)$	$R_L(\Omega \text{ cm}^2)$
2304 duplex steel	9.96	55.24	105	59	189.4	167	4.6
316L stainless steel	5.25	42.14	948	1240	168.2	--	--

**Figure 6.** SEM images of the (a) 2304 duplex and (b) 316L austenitic stainless steel rebar

In Table 3, the values of the modeling elements are shown using the equivalent circuits of the figure 4. As shown in this table, the charge transfer resistance as the main element was  $59 \Omega$  for austenitic steel. However, the charge transfer resistance for 316L austenitic stainless steel was  $1240 \Omega$ , which is relatively high. Compared to  $CPE_f$  and  $CPE_{dl}$ , it is found that  $CPE_f$  is lower than  $CPE_{dl}$  in both rebars which indicates that the formed passive film is thin and the double layer at the interfaces has a high capacitive behavior [24]. Furthermore, the findings indicate that there is a good agreement between the experimental data and the modeling elements.

The top-view SEM images of the 2304 duplex and 316L austenitic stainless steel rebar are shown in Figure 6. The 316L austenitic stainless steel surface is approximately uniform, without evidence of defects/pores and unevenness which can decrease the influence of moisture and aggressive ions on the surface from the environment. Furthermore, selected microstructure of the austenitic

stainless steel presents that no porosity is observed in the surface of the steel, which results in very high densification of the materials.

#### 4. CONCLUSION

Reinforcement corrosion in concrete structures leads to serious damages that reduce the service life of structures. In this research, corrosion resistance of stainless steel reinforced concretes exposed to a corrosive environment were investigated using electrochemical techniques. In order to describe corrosion behavior of the stainless steel reinforced concretes, EIS, OCP and potentiodynamic polarization tests were performed after 60 min exposure time. The corrosion current density of the 316L austenitic and 2304 duplex steels were 0.052 and 0.063  $\mu\text{A}/\text{cm}^2$ , respectively, which were determined by potentiodynamic polarization diagrams. Nyquist diagram of the 316L austenitic stainless steel rebar indicates only an incomplete capacitive semi-circle, indicating the formation of a passive layer with a high protective property. An inductive behavior at high frequency was observed for 2304 duplex steel. The SEM image of the 316L austenitic stainless steel indicates that no porosity was observed in the surface of the steel, which results in a very high densification of the materials.

#### References

1. C.G. Berrocal, K. Lundgren and I. Löfgren, *Cement and Concrete Research*, 80 (2016) 69.
2. P. Shao, L. Ding, J. Luo, Y. Luo, D. You, Q. Zhang and X. Luo, *ACS applied materials & interfaces*, 11 (2019) 29736.
3. V. Volpi-León, L. López-León, J. Hernández-Ávila, M. Baltazar-Zamora, F. Olguín-Coca and A. López-León, *International Journal of Electrochemical Science*, 12 (2017) 22.
4. Q. Liu, B. Chen and Y. Li, *International Journal of Electrochemical Science*, 11 (2016) 10238.
5. C. Li, S. Hu, L. Yang, J. Fan, Z. Yao, Y. Zhang, G. Shao and J. Hu, *Chemistry—An Asian Journal*, 10 (2015) 2733.
6. G. Duffó, S. Farina and F.S. Rodríguez, *Construction and Building Materials*, 210 (2019) 548.
7. Y. Zhang, *International Journal of Electrochemical Science*, 14 (2019) 9347.
8. L. Yang, G. Yi, Y. Hou, H. Cheng, X. Luo, S.G. Pavlostathis, S. Luo and A. Wang, *Biosensors and Bioelectronics*, 141 (2019) 111444.
9. P. Shao, X. Duan, J. Xu, J. Tian, W. Shi, S. Gao, M. Xu, F. Cui and S. Wang, *Journal of hazardous materials*, 322 (2017) 532.
10. C. Van Niejenhuis, S. Walbridge and C. Hansson, *Journal of materials science*, 51 (2016) 362.
11. G. Cao, L. Wang, Z. Fu, J. Hu, S. Guan, C. Zhang, L. Wang and S. Zhu, *Applied Surface Science*, 308 (2014) 38.
12. J. Chen and X. Zhang, *International Journal of Electrochemical Science*, 12 (2017) 5036.
13. J. Hu, C. Zhang, B. Cui, K. Bai, S. Guan, L. Wang and S. Zhu, *Applied Surface Science*, 257 (2011) 8772.
14. G. Ruhi, O. Modi and I. Singh, *Corrosion Science*, 51 (2009) 3057.
15. J. Rouhi, C.R. Ooi, S. Mahmud and M.R. Mahmood, *Materials Letters*, 147 (2015) 34.
16. R. Antunes, M. De Oliveira and I. Costa, *Materials and Corrosion*, 63 (2012) 586.
17. S. Kakooei, J. Rouhi, E. Mohammadpour, M. Alimanesh and A. Dehzangi, *Caspian Journal of Applied Sciences Research*, 1 (2012) 16.



18. W. Zhao, J. Zhao, S. Zhang and J. Yang, *International Journal of Electrochemical Science* 14 (2019) 8039.
19. A.T. Yousefi, S. Ikeda, M.R. Mahmood, J. Rouhi and H.T. Yousefi, *World Applied Sciences Journal*, 17 (2012) 524.
20. H.E. Jamil, M. Montemor, R. Boulif, A. Shriri and M. Ferreira, *Electrochimica acta*, 48 (2003) 3509.
21. A. Hermas and M. Morad, *Corrosion Science*, 50 (2008) 2710.
22. M. Husairi, J. Rouhi, K. Alvin, Z. Atikah, M. Rusop and S. Abdullah, *Semiconductor Science and Technology*, 29 (2014) 075015.
23. H.-S. Lee, J.-H. Park, J. Singh and M. Ismail, *Materials*, 9 (2016) 753.
24. B. Li, Y. Huan and W. Zhang, *International Journal of Electrochemical Science*, 12 (2017) 10402.

© 2020 The Authors. Published by ESG ([www.electrochemsci.org](http://www.electrochemsci.org)). This article is an open access article distributed under the terms and conditions of the Creative Commons Attribution license (<http://creativecommons.org/licenses/by/4.0/>).